Journal of the Ceramic Society of Japan 121 [8] 598-601 2013 Paper

Oxygen vacancies in $PbTiO_3$ thin films probed by resonant Raman spectroscopy

Ken NISHIDA,† Minoru OSADA,* Joe SAKAI, Nobuaki ITO,*** Takashi KATODA,**** Rikyu IKARIYAMA,***** Hiroshi FUNAKUBO,***** Hiroki MORIWAKE****** and Takashi YAMAMOTO**

Department of Communications Engineering, National Defense Academy, Yokosuka, Kanagawa 239–8686, Japan
*International Center for Materials Nanoarchitectonics, National Institute for Materials Science, Tsukuba, Ibaraki, 305–0044, Japan
**Laboratoire GREMAN, UMR 7347 CNRS, Université François Rabelais de Tours, Parc de Grandmont 37200 Tours, France
***Center for Nano Materials and Technology, Japan Advanced Institute of Science and Technology, Nomi, Ishikawa 923–1292, Japan
****Department of Electronic and Photonic Engineering, Kochi University of Technology, Kami, Kochi 780–8502, Japan
*****Department of Innovative and Engineered Materials, Tokyo Institute of Technology, Yokohama 226–8502, Japan
******Nanostructures Research Laboratory, Japan Fine Ceramics Center, Nagoya 456–8587, Japan

Resonant Raman spectroscopy was applied to evaluate oxygen vacancies in $PbTiO_{3-x}$ thin films that were heat treated in a hydrogen atmosphere at various temperatures. Additional mode related to oxygen vacancies occurred in the resonant Raman measurement condition, and its intensity was in proportion to the oxygen vacancy concentration. This correlation offers a simple and useful probe for oxygen vacancies in oxide-based devices.

Key-words : $PbTiO_3$ thin films, Oxygen vacancy, Heat treatment, Resonant Raman spectroscopy, Photoluminescence, Non-Rutherford elastic resonance scattering

[Received April 15, 2013; Accepted April 29, 2013]

1. Introduction

Due to the excellent dielectric, pyroelectric, piezoelectric, and ferroelectric properties,[1)–3)] Pb-based ferroelectric materials such as $PbTiO_3$ and $Pb(Zr,Ti)O_3$ with perovskite-type structures are very successful in electric device applications, including infrared radiation sensors, microactuators, and nonvolatile memories. However, Pb or oxygen vacancies frequently occur during crystal growth or device fabrication because Pb and their oxides have high vapor pressures. These vacancies affect the ferroelectric properties such as degradation of the insulation property or pinning of polarization switching.[4)–8)] Pb or oxygen vacancies have been evaluated in bulk materials using X-ray diffraction or neutron radiation, and thermogravimetry.[9),10)] Additionally, the relationship between vacancy concentration and properties has been discussed.[9)]

As electronic devices become highly integrated and miniaturized, the importance of thin film applications using ferroelectric materials has increased. Unfortunately, methods used to evaluate vacancies in the bulk are not applicable to films because films have a much smaller absolute amount of vacancies compared to the bulk. Although X-ray fluorescence (XRF) can evaluate Pb vacancies in $PbTiO_3$ with a relatively high sensitivity and reliability even in films, detecting oxygen vacancies in oxides is quite difficult.

Only a few reports have evaluated oxygen vacancies in perovskite-type oxide films. The oxygen vacancies of a $SrRuO_3$ thin film and other materials have been reported using a non-Rutherford elastic resonance scattering (NRERS) method.[11),12)] However, NRERS has some disadvantages; the equipment is expensive, the spatial resolution is limited to ~mm scale, and samples are occasionally damaged during measurements.

Raman spectroscopy is a versatile, highly sensitive technique used to evaluate the crystal structure. Additional advantages include a relatively high spatial resolution and a nondestructive measurement without direct specimen contact. Moreover, the phase transition and identification of the substitution site in ferroelectric materials have been reported using Raman spectroscopy analysis.[13),14)] Although Raman spectroscopy is a powerful tool for crystal structure evaluations, reports on the film defects such as oxygen vacancies are limited.

We have employed polarized Raman spectroscopy to evaluate oxygen vacancies in epitaxial $PbTiO_3$ thin films.[15)–17)] Herein a resonant Raman spectroscopy technique is applied as a highly sensitive and accurate method to evaluate oxygen vacancies. An additional mode related to oxygen vacancies is dominant in the resonant Raman measurement condition. The intensity of this additional mode increases as the oxygen vacancy concentration increases. The relationship between Raman intensity of the additional phonon mode and oxygen vacancies is used to estimate the oxygen content in $PbTiO_3$ thin films.

2. Experimental procedure

Metal organic chemical vapor deposition (MOCVD) was used to grow 300–400 nm thick $PbTiO_3$ thin films on (100) MgO substrates. The details of the growth conditions are described elsewhere.[18)] High-resolution X-ray diffraction (XRD) measurements (PANalytical, X'Pert MRD) confirmed epitaxial growth of $PbTiO_3$ thin films with a (001)/(100) orientation. Various oxygen vacancy concentrations were generated by heat treatment of

† Corresponding author: K. Nishida; E-mail: nishida@nda.ac.jp

DOI http://dx.doi.org/10.2109/jcersj2.121.598

$PbTiO_3$ thin films between 600–800°C for two hours under a hydrogen atmosphere. X-ray fluorescence (XRF) spectroscopy (Philips, PW2404) determined the Pb/Ti ratio in the films. The NRERS method using Rutherford backscattering (RBS) equipment (Nissin high oxygen vacancyltage Co., NH-1700) was used to estimate the absolute content of oxygen vacancies in $PbTiO_3$ thin films (actual oxygen ion content in $PbTiO_3$ thin films).

Raman spectra were measured using micro-Raman system. An Ar + Kr mixed gas ion laser was used as an excitation source capable of changing its emission wavelength from 488.0 to 647.1 nm. The laser probe beam was focused on surface spot measuring 1 μm in diameter through a 100× objective lens with NA = 0.75. Backward scattered light was collected and dispersed by a subtractive triple spectrometer (Jobin Yvon T64000) with a fixed measurement time of 60 s.

3. Results and discussion

$PbTiO_3$ belongs to the C_{4v} space group, which yields $3A_1 + B_1 + 4E$ phonon modes.[19),20)] Polarized Raman analysis was performed to identify the phonon modes in the Raman spectra. In addition to displaying all expected phonon modes, the Raman spectra of $PbTiO_3$ films demonstrate a typical tetragonal phase without a secondary phase, indicating high quality samples are produced.

Figure 1 shows the *yy*-polarized Raman spectra for $PbTiO_3$ thin films heat-treated at 700°C under a hydrogen atmosphere with incident light of various wavelengths from 488.0 to 647.1 nm. The intensity of Raman spectra was normalized by that from Si single crystal. The Pb content of this film remains nearly constant, but the oxygen content decreases by 9%, as discussed later. The Raman spectra of the $PbTiO_3$ thin film exhibits the typical *yy*-polarized property based on the Raman selection rule; A_1(TO) symmetry and B_1-phonon modes are observed. As shown in the inset, an additional mode related to the oxygen vacancies (~289 cm^{-1}) occurs at the lower frequency side of the B_1-phonon mode around 293 cm^{-1}. The peak of additional phonon mode and B_1-phonon mode were illustrated in the inset of Fig. 1 as Lorenz Function shape. First principles calculations of a $PbTiO_3$ model with oxygen vacancies support the assignment of the additional mode. The additional phonon mode was disappeared with re-oxidized treatment. These results are going to be reported in another paper.[21)] The Raman peak of the additional mode is predominant when the excitation is 520.8 or 568.2 nm, but decreases with laser excitation at 647.1 nm.

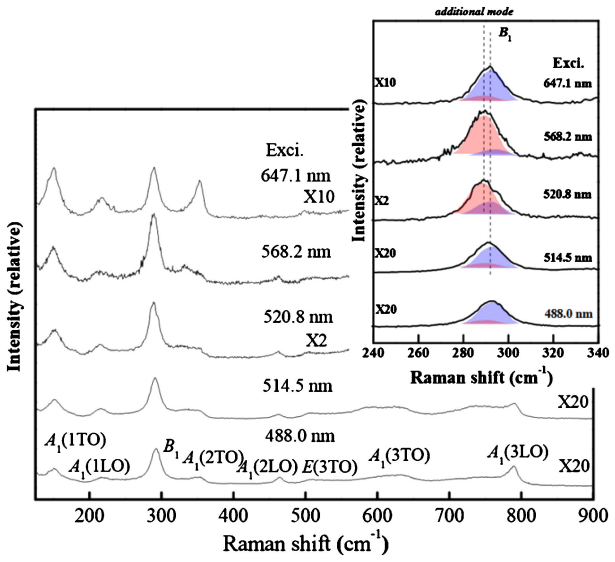

Fig. 1. *yy*-polarized Raman spectra of $PbTiO_3$ thin films heat treated at 700°C. Wavelength of the excitation laser changed from 488.0 to 568.2 nm. Inset shows an enlarged view of the spectra around 300 cm^{-1}.

Figure 2(a) shows the photoluminescence (PL) spectra of $PbTiO_3$ thin films before and after heat treatment at 700°C. Heat treatment shifts the PL peak position from 560 to 570 nm. Because heat treatment generates oxygen vacancies, the emission related to the oxygen vacancies becomes dominant. The emission energy that transits from the oxygen vacancy–related deep donor to the conduction band agrees well with a previous report.[22)]

Figure 2(b) shows the dependence of the Raman scattering intensity on the incident laser wavelength. The peak intensity of the additional mode increases with the excitation laser wavelength until about 570 nm and then decreases; the additional mode intensities excited at 520.8 and 568.2 nm are about 5 and 18 times larger than that at 488.0 nm, respectively. The dependence of the additional mode intensity in the Raman spectrum on excitation wavelength agrees well with the PL intensity of a $PbTiO_3$ thin film heat-treated at 700°C. Due to this coincidence, the incident laser wavelength (energy) dependence by Raman scattering in resonance with transitions is involved in the recombination process of the oxygen vacancy band. It should be noted that the resonance effect successfully evaluates the oxygen vacancy.

Figure 3 shows the *yy*-polarized Raman spectra for $PbTiO_3$ thin films before and after heat treatment from 600 to 800°C. Based on the results shown in Fig. 2(b), the wavelength of the excitation laser was fixed at 568.2 nm, which is the resonant condition for oxygen vacancies. The additional phonon mode was predominant in this condition. The intensity of the additional phonon mode increases as the heat treatment temperature increases, indicating the intensity of the additional phonon mode increases with the oxygen vacancy content.

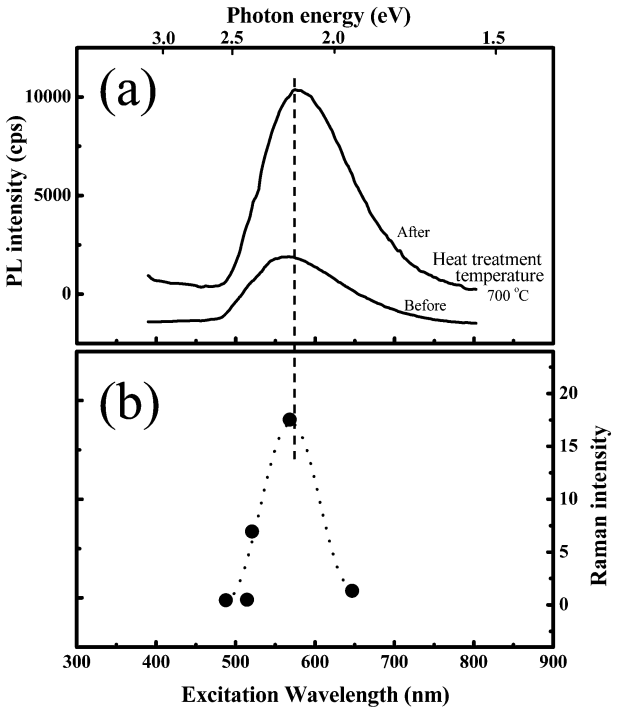

Fig. 2. (a) PL spectrum of $PbTiO_3$ thin films before and after heat retreatment at 700°C and (b) Raman intensity of the additional mode peak as a function of excitation laser wavelength.

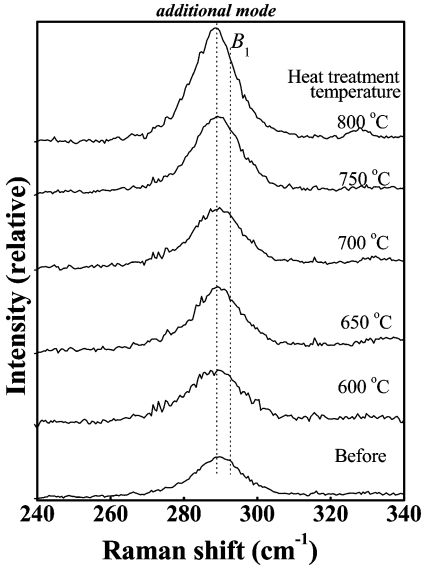

Fig. 3. *yy*-polarized Raman spectra of $PbTiO_3$ thin films heat-treated at various temperatures. Wavelength of excitation laser is fixed at 568.2 nm.

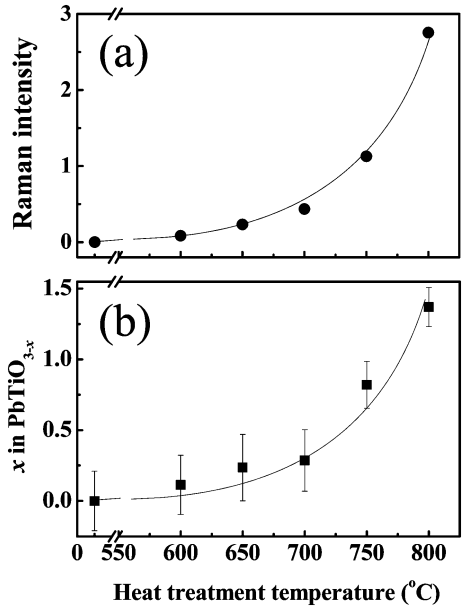

Fig. 4. (a) Raman peak intensity of the additional mode as a function of heat treatment temperature. (b) x in $PbTiO_{3-x}$ determined by NRERS as a function of heat treatment temperature.

Figure 4(a) plots the intensity of the additional phonon mode based on before heat-treated $PbTiO_3$ thin film versus heat treatment temperature using the data shown in Fig. 3. The intensity of the additional phonon mode slightly increases as heat treatment temperature increases until 700°C, but dramatically increases above 750°C. Figure 4(b), which plots the dependency of the heat treatment temperature on the x value in $PbTiO_{3-x}$ determined by NRERS, shows that the x value in $PbTiO_{3-x}$ thin films increases as the heat treatment temperature increases.

Figure 5 plots the intensity of the additional phonon mode as a function of the x value in $PbTiO_3$. The intensity of the additional phonon mode monotonically increases as the x value increases. A good correlation is observed between the intensity of the

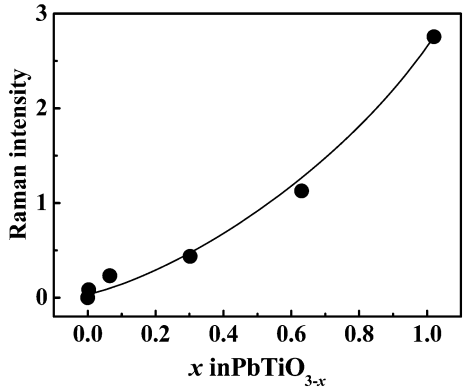

Fig. 5. Relationship between Raman peak intensity of the additional mode and x in $PbTiO_{3-x}$.

additional phonon mode and the oxygen ion content in $PbTiO_3$ thin film. Thus, resonant Raman spectroscopy can evaluate the oxygen vacancies in $PbTiO_3$ thin films with a high sensitivity and accuracy even if the oxygen vacancy concentration is low, e.g., for films heat-treated below 700°C, which are hardly detected by NRERS. The result shown in Fig. 4 is a very useful guideline to determine the concentration of oxygen vacancies x in $PbTiO_{3-x}$ using Raman resonant spectroscopy.

4. Summary

In summary, oxygen vacancies in $PbTiO_3$ thin films can be evaluated by resonant Raman spectroscopy. The intensity of the additional mode, which is related to oxygen vacancies, increases as the oxygen vacancy content increases, even if the content is quite small. This relationship is a useful guideline to determine the amount of vacancies (x in $PbTiO_{3-x}$ thin films). These results indicate that resonant Raman spectroscopy is a versatile, highly sensitive, and accurate tool to evaluate crystal structure.

References

1) J. F. Scott and C. A. Araujo, *Science*, **246**, 1400–1405 (1989).
2) J. S. Wrigh and L. F. Francis, *J. Mater. Res.*, **8**, 1712–1720 (1993).
3) R. Takayama, Y. Tomita, K. Iijima and I. Ueda, *J. Appl. Phys.*, **63**, 5868–5872 (1988).
4) T. Tamura, K. Matsuura, H. Ashida, K. Kondo and S. Otani, *Appl. Phys. Lett.*, **74**, 3395–3397 (1999).
5) J.-P. Han and T. P. Ma, *Appl. Phys. Lett.*, **71**, 1267–1269 (1997).
6) S. Zafar, V. Kaushik, P. Laberge, P. Chu, R. E. Jones, R. L. Hance, P. Zurcher, B. E. White, D. Taylor, B. Melnick and S. Gillespie, *J. Appl. Phys.*, **82**, 4469–4475 (1997).
7) K. Kushida-Abdelghafar, H. Miki, K. Torii and Y. Fujisaki, *Appl. Phys. Lett.*, **69**, 3188–3190 (1996).
8) N. Ikarashi, *Appl. Phys. Lett.*, **73**, 1955–1957 (1998).
9) S. Shirasaki, K. Takahashi, H. Yamamura, K. Kakegawa and J. Mori, *J. Solid State Chem.*, **12**, 84–91 (1975).
10) R. Bittner, K. Humer, H. W. Weber, K. Kundzins, A. Sternberg, D. A. Lesnyh, D. V. Kulikov and Y. V. Trushin, *J. Appl. Phys.*, **96**, 3239–3246 (2004).
11) H. Y. Zhai, Z. H. Zhang and W. K. Chu, *Appl. Phys. Lett.*, **78**, 649–652 (2001).
12) J. Sakai, N. Ito, S. Ito, K. Takahashi and H. Funakubo, *Appl. Phys. Lett.*, **89**, 242115–242118 (2006).
13) K. Nishida, M. Osada, H. Uchida, H. Nakaki, S. Koda, H. Funakubo and T. Katoda, *Jpn. J. Appl. Phys.*, **45**, 7548–7551 (2006).

14) M. Osada, M. Kakihana, S. Wada and T. Noma, *Appl. Phys. Lett.*, 75, 3393–3396 (1999).
15) K. Nishida, H. Kishi, H. Fuakubo, H. Takeuchi, T. Katoda and T. Yamaoto, *Jpn. J. Appl. Phys.*, 46, 7005–7007 (2007).
16) K. Nishida, M. Osada, H. Takeuchi, I. Yosiaki, J. Sakai, N. Ito, R. Ikariyama, T. Kamo, T. Fujisawa, H. Funakubo, T. Katoda and T. Yamamoto, *Jpn. J. Appl. Phys.*, 47, 7510–7513 (2008).
17) K. Nishida, H. Kishi, M. Osada, H. Funakubo, M. Nishide, H Takeuchi, T. Katoda and T. Yamamoto, *Jpn. J. Appl. Phys.*, 48, 09KF11–09KF15 (2009).
18) K. Nagashima, M. Aratani and H. Funakubo, *Jpn. J. Appl. Phys. Part 2*, 39, L996–L998 (2000).
19) C. M. Foster, Z. Li, M. Grimsditch, S. K. Chen and D. J. Lam, *Phys. Rev. B*, 48, 10160–10167 (1993).
20) G. Burns and B. A. Scott, *Phys. Rev. B*, 7, 3088–3101 (1973).
21) K. Nishida, M. Osada, J. Sakai, N. Ito, T. Katoda, R. Ikariyama, H. Funakubo, H. Moriwake and T. Yamamoto, under contribution.
22) Z. Zhang, P. Wua, L. Lu and C. Shu, *Appl. Phys. Lett.*, 88, 142902–142905 (2006).